Synthesis of hydrogel nanocomposites and their application in removing dyes and impurities

Rajabali Ebrahimi[1), *)] (ORCID ID: 0000-0002-4290-8565), **Mahboubeh Taherkhani**[1)] (0000-0002-4539-5937)

DOI: https://doi.org/10.14314/polimery.2023.5.5

Abstract: Polyacrylate hydrogels containing starch, ZnSe and Fe_3O_4 nanoparticles were obtained. The polymerization process was carried out in an ultrasonic field. The structure (SEM, FTIR, XRD), swelling properties and the ability of hydrogels to adsorb dyes (methylene blue, methyl orange, methyl red and Eriochrome Black T) and heavy metals (Cu^{2+}) from wastewater were investigated. Hydrogels containing AgCl nanoparticles were also obtained, which, due to their antibacterial properties, can be potentially used in medicine.

Keywords: acrylic hydrogel, nanocomposites, sonification, heavy metals and dyes adsorption.

Synteza nanokompozytów hydrożelowych i ich zastosowanie do usuwania barwników i zanieczyszczeń

Streszczenie: Otrzymano hydrożele poliakrylanowe zawierające nanocząstki skrobi, ZnSe i Fe_3O_4. Proces polimeryzacji prowadzono w polu ultradźwiękowym. Zbadano strukturę (SEM, FTIR, XRD), właściwości pęczniejące oraz zdolność hydrożeli do adsorpcji barwników (błękit metylenowy, oranż metylowy, czerwień metylowa i czerń eriochromowa T) oraz metali ciężkich (Cu^{2+}) ze ścieków. Otrzymano również hydrożele zawierające nanocząstki AgCl, które ze względu na właściwości antybakteryjne mogą znaleźć potencjale zastosowanie w medycynie.

Słowa kluczowe: hydrożele akrylowe, nanokompozyty, sonifikacja, adsorpcja metali ciężkich i barwników.

Hydrogels have a wide range of applications in various fields i.e., medicine, pharmaceuticals, agriculture, wastewater treatment, manufacturing of technical and electronic units, and as absorbents for pollutant removal in environmental applications [1]. The most outstanding characteristics of these compounds are their biocompatibility, biodegradability, convenient operation, high yield, simplicity of synthesis, ease of use, abundance of primary materials and availability of functional groups [2, 3]. Hydrogels are three-dimensional polymer networks having high absorption capacity of water or biological fluids. These compounds can absorb water even more than 1000 times their mass. The ability of hydrogels to absorb water comes from the hydrophilic functional groups in the polymer chains, including carboxyl –COOH, amino $–NH_2$, hydroxy –OH, sulfonic $–SO_3H$, and amide –CONH groups, while their resistance to dissolution is due to the cross-links between the network chains [4]. In the last two decades, synthetic hydrogels have gradually replaced natural hydrogels due to their long-life, high absorption capacity, and high gel strength. Removal of the solvent from the pores during drying generates capillary forces that lead to the concentration of the gel network. Xerogel is obtained by drying and is in the form of a powder. Sometimes such a gel powder has superior properties in terms of both swelling and reactivity to the absorbed materials but is difficult to prepare. The hydrogel filters and super porous filters can be used to absorb heavy metal pollution, synthetic dyes, petroleum substances and industrial oil wastes. Hydrogel nanocomposites have the highest swelling in pure water and the lowest swelling under pressurized conditions [5, 6].

Silver chloride (AgCl) is a white crystalline solid that is famous for its low solubility in water. It occurs in the nature as the mineral – chlorargyrite. When exposed to sunlight or heating, AgCl decomposes into chlorine gas and metallic silver, which gives the substance a dark color. The unit cell of silver chloride crystals is cube-shaped (FCC) in which each Ag^+ ion is surrounded by an octahedron with six chloride ligands. Silver nanoparticles may contain silver oxide [7]. Nowadays, strong antibacterial activity is the main direction of nanosilver expansion in the field of health. Silver nitrate is usually used in the production of silver nanoparticles. When the nanoparti-

[1)] Department of Chemistry, Takestan Branch, Islamic Azad University, Takestan, Iran.

[*)] Author for correspondence: ra.ebr@iau.ac.ir, pr_ebrahimi_r@yahoo.com

cles are formed, the color of the mixture changes to gray. Centrifuge is used for separation, and distilled water is used for washing colloidal nanoparticles [8].

Ultrasound is sound waves with a frequency above 20 kHz (the upper limit of human hearing). Cavitation is the main phenomenon that occurs during the action of ultrasound in chemical processes where voids are created in the liquid because of high vacuum. With cavitation, not only physical stirring and homogenization takes place, but sometimes the necessary activation energy is also provided for chemical reactions. These two effects in some cases occur simultaneously and thus lead to remarkable results [3]. Strong ultrasound might convert monomeric aqueous solution to semi-solid and stable hydrogel. This is done only in a viscous environment such as glycerin. Glycerin increases viscosity and therefore the formation of free radicals resulting from ultrasonic cavitation. Besides, the solubility of the polymer is reduced, and the degradation reaction is delayed. In the aqueous environment, ultrasounds destroy the gel and liquefy it into an aqueous solution [9, 10].

Nanocomposite hydrogels have been found to be useful for water purification [11]. Carboxymethylcellulose (CMC)/poly(3-sulfopropyl methacrylate) hydrogel was used to remove methylene blue [12]. Absorption of methylene blue from aqueous solution was also evaluated using a beta-cyclodextrin/zinc oxide composite. The lowest absorption was observed at neutral pH 7 whereas, the highest was observed acidic pH 1. The absorption was done quickly in 15 minutes, and the equilibrium was reached after 30 minutes. The highest absorption capacity was occurred at the temperature of 20°C, at the concentration of 5 mg/L of the pollutant in the presence of 0.005 g/L of the adsorbent [13]. Fe_3O_4-g-PAA magnetic nanocomposite hydrogel has been synthesized through radical polymerization in the presence of methylenebisacrylamide (MBA), as cross-linker, and has resulted in an adsorbent with a removal capacity of 507.7 mg/g for methyl blue [14]. Khan et al reported a Guar gum adsorbent hydrogel combined with zinc oxide nanoparticles proper for removing chromium (VI) from water. ZnO nanoparticles improved the recovery of the adsorbent from the aqueous solution after the removal of chromium (VI) [15]. The advantage of ZnO-modified CMC hydrogel is low cost, ability to absorb dyes and antibacterial activity [16]. Moreover, PAAm/CS/Fe_3O_4 hydrogel composite was used to remove methylene blue from the aqueous solution [17]. Sodium alginate/ZnO hydrogel nanocomposite, compared to pure hydrogel, showed high thermal stability and excellent recycling performance. The incorporation of zinc oxide nanoparticles in the hydrogel matrix increased the swelling capacity and decreased the mechanical strength [18]. CMC/PPA hydrogel nanocomposites containing carboxyl and hydroxyl functional groups were reinforced with graphene oxide to obtain non-toxic and environmentally friendly absorbent, effective in multiple removal ionic pollutants from wastewater. The pore size of the nanocomposites decreases as graphene oxide concentration increases. These hydrogels have the capacity to absorb 138 mg/g of methylene blue after 4 h [19]. Moreover, nanocomposites based on silver nanoparticles coated with 4-amino-N-tetradecyl pyridinium bromide and silica gel were used to remove copper(II) ions from aqueous solution. The maximum copper(II) ions removal, equaling to 98.6%, was obtained using 0.4 g of the nanocomposite, suggesting high efficiency in removing copper(II) ions [20].

The aim of these studies was the absorption of certain substances, the removal of impurities from the aqueous solution and the implementation of silver chloride nanoparticles in gel holes for the first time. For this purpose, acrylic hydrogel, and some of its nanocomposites (containing starch and Fe_3O_4, ZnSe nanoparticles) were synthesized by sonification and their swelling was also studied. The ultrasonic polymerization procedure described herein has some applications where initiators and heat are not desirable.

EXPERIMENTAL PART

Materials

All the materials and chemicals utilized in this work are of analytical grade, were obtained from Merck company, and they are used without further purification.

Double distilled water and pure glycerin as solvent, acrylic acid (AA) and acrylamide (AAM) as monomer and methylenebisacrylamide (MBA) as crosslinker, potassium dihydrogen phosphate (KH_2PO_4), sodium hydrogen phosphate (Na_2HPO_4) for making buffer solutions, sodium hydroxide (NaOH) for neutralizing acrylic acid, and starch for preparing a hydrogel composite were all purchased from Merck, Germany; and Fe_3O_4 and ZnSe nanoparticles were synthesized.

Synthesis of hydrogels

1.5 g of AAM, 1.5 g of AA, 0.2 g of MBA and 0.2 g of NaOH were added to 24 g of glycerin and water in a 20 mL beaker. For some samples, 0.2 g of starch, Fe_3O_4 or ZnSe were also added at the last stage [1]. The resulting mixture was stirred using a magnetic stirrer (Heidolph Instruments, Germany) and then sonicated (20 kHz, 56 W) using ultrasonic probe (Brandlin Electronic GmbH, Germany). The gelation process lasted about 5 minutes. The product was crushed in a mortar and washed successively with distilled water at room temperature (200 mL), hot water (200 mL) and ethanol (200 mL) for one hour each time. After filtration, the sample was oven dried at 70°C for 8 h (INB400, Memmert GmbH, Germany). The dried hydrogel was ground in a mortar and the resulting powder was stored in a container.

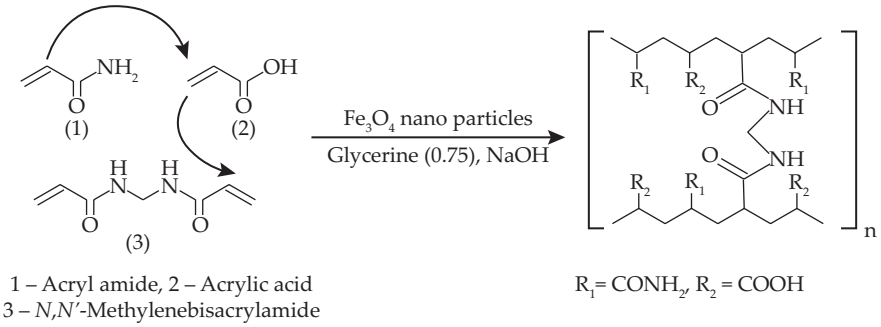

Fig. 1. Mechanism of the cross-linking reaction

Synthesis of silver chloride nanoparticles inside gel cavities

The synthesis of silver chloride nanoparticles inside the gel cavities was done by three different, innovative methods. In the first method, 10 mL of silver nitrate solution (0.085 g/L) and 10 mL of sodium chloride solution (0.05 g/L) were mixed with 0.05 g of hydrogel for 1 h. The swollen gel was washed with distilled water and ethanol. After drying for 24 h at 70°C, the gel was placed in a special container. The presence of silver chloride absorbed in the cavities of the hydrogel was determined by SEM. In the second method 10 mL of silver nitrate solution (0.085 g/L) was added to 0.05 g of hydrogel, stirred for 60 min, and washed with distilled water. Then, 10 mL of sodium chloride solution (0.05 g/L) was added and stirred for another 60 min.–Thereafter, filtration, washing and drying were carried out, as in the first method. In the third method 10 mL of sodium chloride solution (0.05 g/L) was added to 0.05 g of hydrogel. After being stirred for 60 min, filtrated, and washed, 10 mL of silver nitrate solution (0.085 g/L) was added, and all the steps of washing, drying, and grinding were repeated like the previous. SEM confirmed silver chloride absorption.

Methods

Dye solutions of methyl orange, methyl red, methylene blue and Eriochrome Black T were selected, which showed appropriate and specific spectra in the UV-VIS range. Each solution was diluted several times to determine the optimal working concentrations. 5 g of methylene blue was added to a 100 mL flask and diluted 20-fold, then the UV absorption was measured using UV device (8453, Agilent, USA). 0.05 g of a simple hydrogel and 25 mL of a methylene blue solution at a concentration of 9.76 mg/L were mixed using a magnetic stirrer (1250 rpm). After 130 seconds, part of the solution was centrifuged (3500 rpm) and then its UV absorbance was measured. These steps were repeated several times during mixing. The same procedure was repeated with other hydrogels. Then, the absorption of 25 mL of methyl orange 78.125 mg/L by 0.05 g of Fe_3O_4 hydrogel, the absorption of 25 ml of Eriochrome Black T 19.5 mg/L by 0.05 g of simple hydrogel and 0.05 g of starch hydrogel, and the absorption of 50 ml of methyl red 78.125 mg/L by 0.1 g starch hydrogel powder were measured.

The FT-IR analysis was carried out on a spectrophotometer (RX1, Perkin Elmer, USA), with a scanning range between 4000 and 400 cm^{-1} at room temperature (27°C). Scanning electron microscope (SEM, XL30, Philips, Netherlands) and X-ray (D8, Bruker, USA) images were used to study the morphology of prepared hydrogels surfaces.

RESULTS AND DISCUSSION

Hydrogel formation

For the synthesis of hydrogels by ultrasound, the required amounts of water, glycerin, acrylamide, and acrylic acid were homogenized with a magnetic stirrer, and then methylene bisacrylamide was added to the mixture as a cross-linking agent. After adding sodium hydroxide, the mixture was sonicated to produce a hydrogel. For the preparation of other hydrogels, sufficient

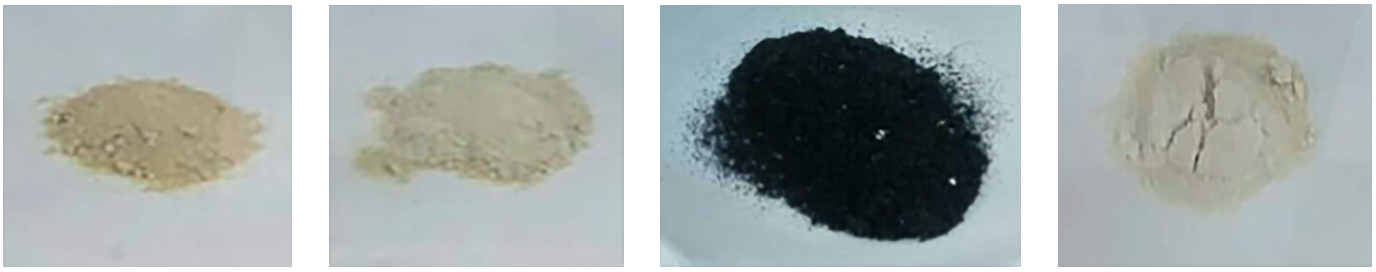

Simple gel | Starch/Gel | Fe_3O_4/Gel | ZnSe/Gel

Fig. 2. Pictures of the obtained hydrogels

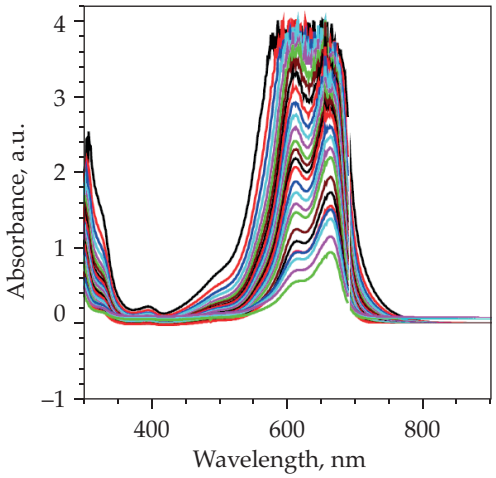

Fig. 3. UV spectra of diluted methylene blue solutions in 30 steps

starch or Fe_3O_4 or ZnSe nanoparticles were added before ultrasonic treatment. The sonication time was 168 s for simple gel, 124 s for starch/gel and 104 s for Fe_3O_4/gel. In the case of ZnSe, the gel formed at room temperature only after 2 h and was stronger and stiffer than the others. Figure 1 shows the mechanism of the cross-linking reaction. The obtained hydrogels are shown in Figure 2.

The gel formation efficiency

The gel formation efficiency was calculated using equation 1. The results are shown in Table 1. The highest and lowest process efficiency is related to Fe_3O_4/gel and simple gel, respectively. The presence of an additive, particularly nanoparticles, significantly increases the efficiency of gel formation.

$$\text{Gel formation efficiency} = M_g/M_i \cdot 100 \quad (1)$$

where: M_g – mass of obtained gel (g), M_i – mass of the initial materials (g)

T a b l e 1. Gel formation efficiency

Gel type	Gel formation efficiency, %
Simple gel	48.25
Starch/gel	50.05
Fe_3O_4/gel	58.95
ZnSe/gel	55.39

Silver chloride nanoparticles were formed inside the gel cavities using three innovative methods: i) silver nitrate and sodium chloride solutions were together added to the gel powder, the solution was slightly cloudy and dark green, and this color was due to the simultaneous effect of silver and chlorine ions on the gel (efficiency 34.5%), ii) first, silver nitrate solution and then sodium chloride solution were added to the powder, the resulting gel powder was cloudy and brownish, which was due to the rapid absorption of silver ions in the gel (32.5%), iii) first, sodium chloride solution and then silver nitrate solution were added to the gel powder, the color of the resulting powder, due to the faster absorption of chlorine ions by the gel, was slightly brighter than the initial gel (41%).

The color solutions absorption

For various concentrations of methylene blue, methyl orange, methyl red and Eriochrome Black T solutions, absorption spectra in the wavelength range of 200–900 nm were measured, and their optimal concentrations were determined. For example, a methylene blue solution was diluted from 5 000 mg/L to 3.792 mg/L in 30 steps (Fig. 3), and a concentration of 78.125 mg/L was selected for quantitative measurements. The specified amount of each gel was added to this solution. After filtration, the absorption of the resulting solution was measured. For methyl red, the optimal concentration was 78.125 mg/L, and for Eriochrome Black T 19.5 mg/L. In Fig. 4, the black line shows the absorption of methyl orange on

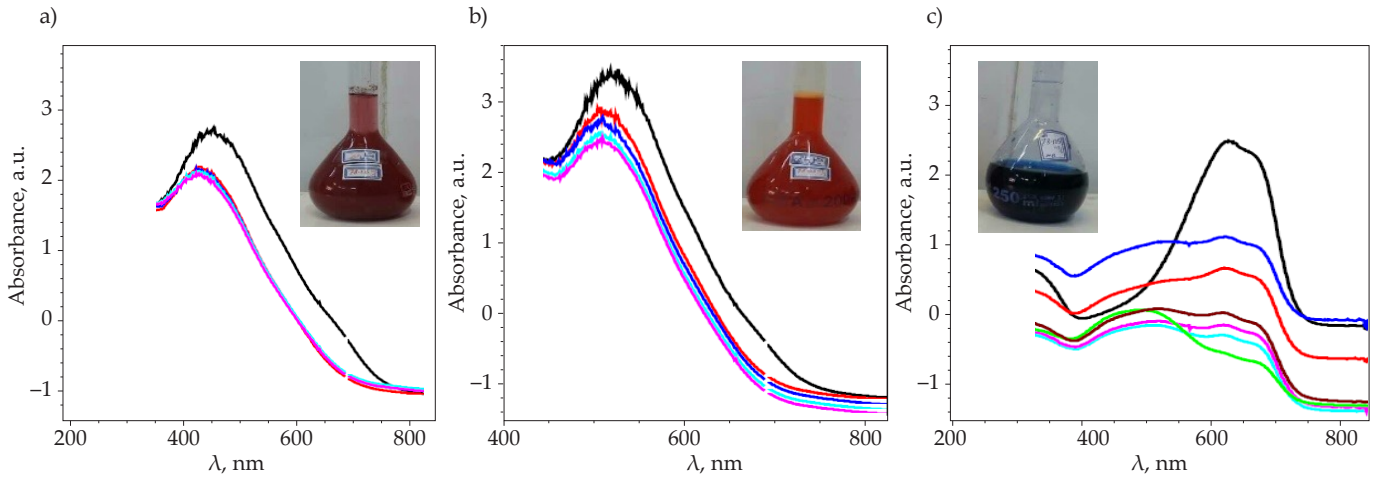

Fig. 4. UV-VIS spectra of dye solutions with and without hydrogels: a) methyl orange on Fe_3O_4/gel, b) methyl red on starch/gel c) Eriochrome black T on starch/gel

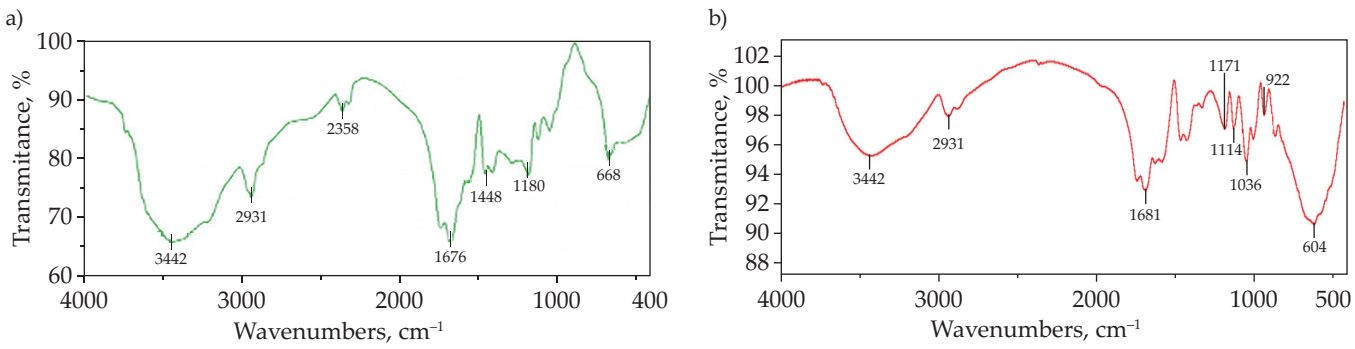

Fig. 5. FTIR spectra of simple hydrogel (a)and ZnSe/gel (b)

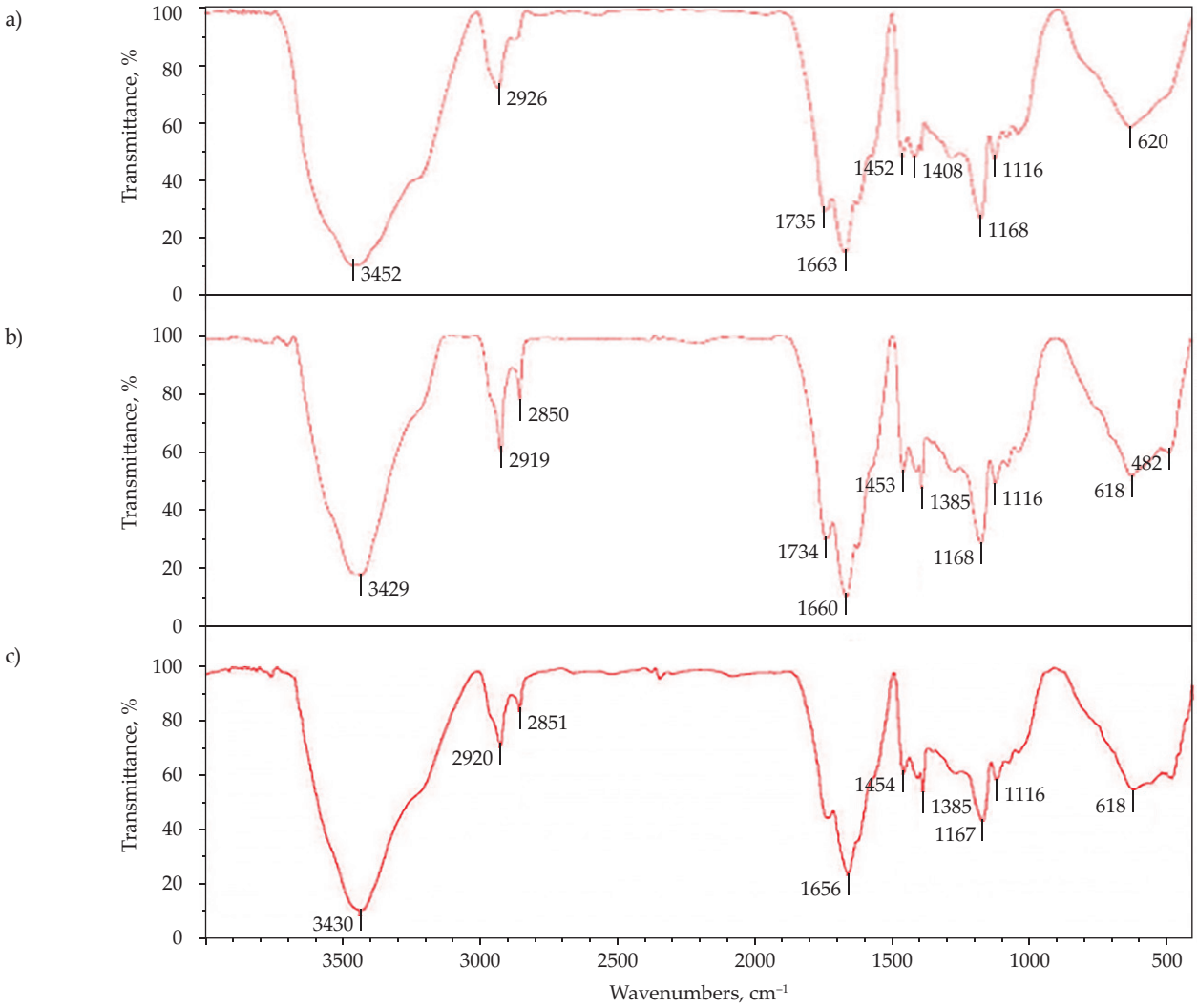

Fig. 6. IR spectra of the hydrogel: a) silver nitrate and sodium chloride were added simultaneously, b) silver nitrate was first added, c) sodium chloride was first added

Fe_3O_4/hydrogel (4a), methyl red on starch/hydrogel (4b) and Eriochrome Black T on starch/hydrogel (4c); the other curves correspond to the spectra of dye solutions without hydrogels (3 to 6 measurements).

IR analysis of hydrogels

In Fig. 5 shows the IR spectra of simple hydrogel and ZnSe/gel. The change in the structure of the hydrogel consists in breaking the methylene bisacrylamide cross-links. The peak at 3442 cm^{-1} corresponds to hydroxyl stretching vibrations and the peak at 2931 cm^{-1} corresponds to symmetrical C-H bond stretching vibrations. The peak at 1675 cm^{-1} is related to the stretching vibrations of the carbonyl or amide group [21].

Fig. 6 shows the IR spectra of silver chloride containing hydrogels. The peak in the range of 3400–3500 cm^{-1} is related to the stretching vibrations of the -OH groups

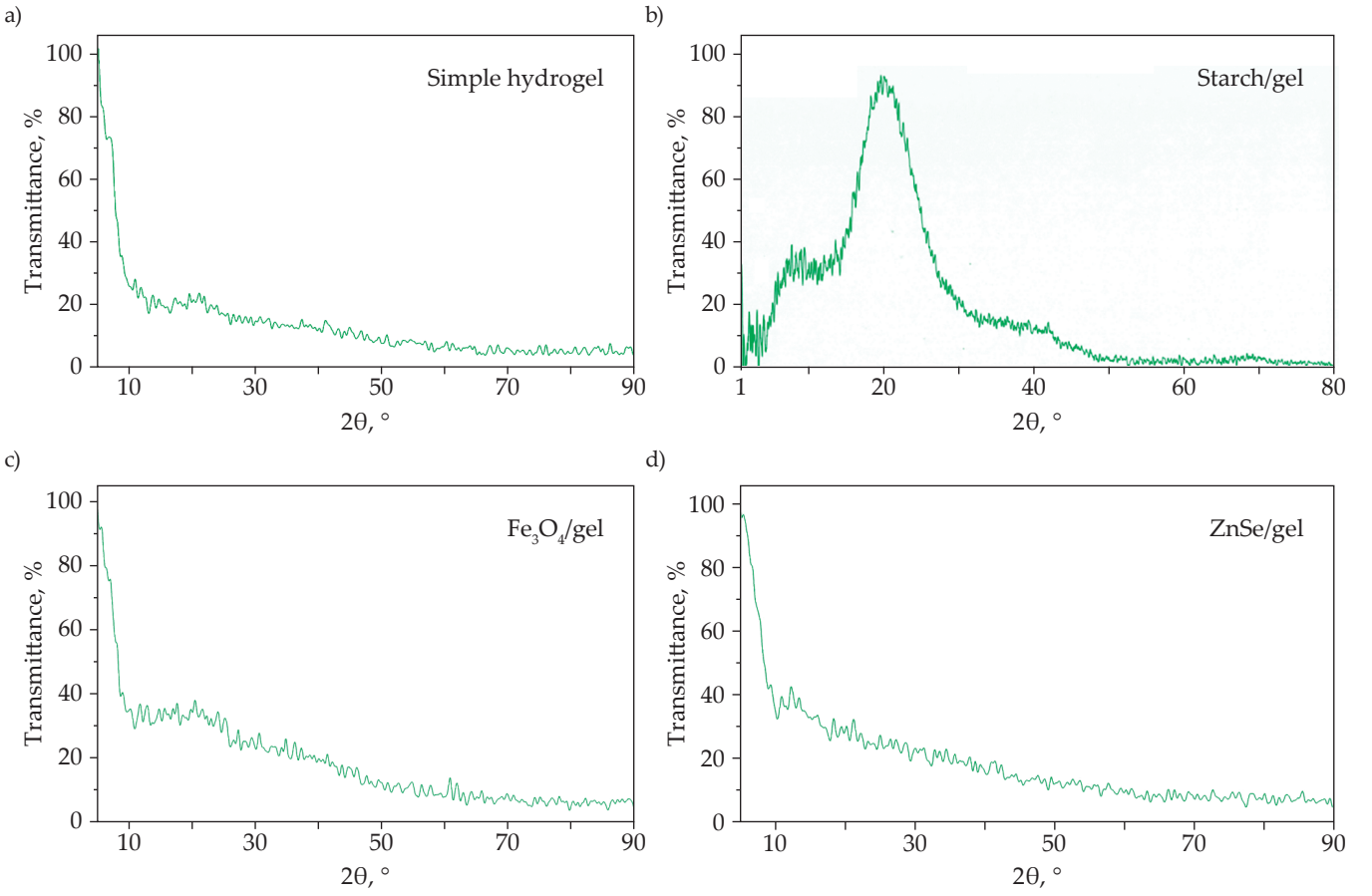

Fig. 7. XRD spectra of simple hydrogel and hydrogels containing starch, Fe_3O_4 and ZnSe. a) Simple hydrogel b) Starch/gel c) Fe_3O_4/gel, d) ZnSe/gel

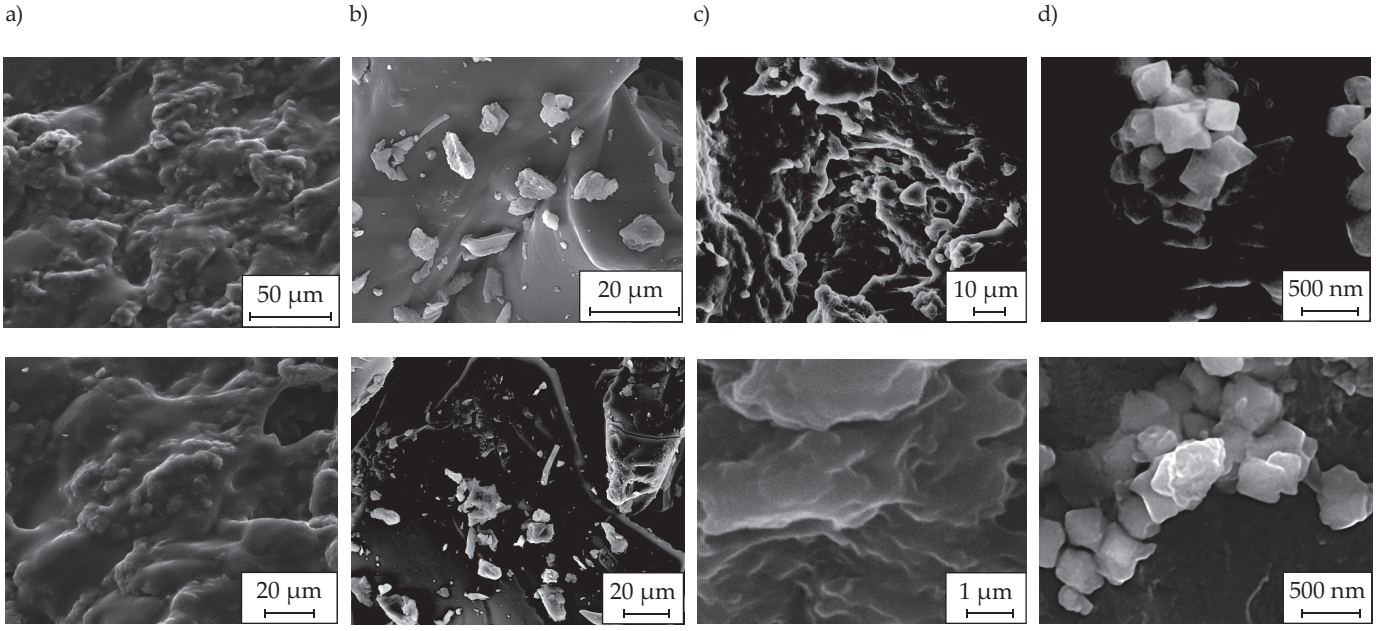

Fig. 8. SEM images of hydrogels: a) simple hydrogel (layered structure), b) hydrogel containing starch (particles inside the gel cavities), c) hydrogel containing ZnSe (layered cavities), and d) hydrogel containing Fe_3O_4 (cubic crystals)

and the vibrations of the amino groups in the chain. The peak at 2919 cm^{-1} corresponds to the symmetrical stretching vibrations of C-H bonds, and the peak at 1734 cm^{-1} corresponds to the stretching vibrations of C=O ketone groups. Peak at 1452 cm^{-1} is associated with vibrations of C-N bonds and peak 1167 cm^{-1} with vibrations of C-C bonds. In addition, in the region of 618 cm^{-1}, a peak associated with C-Cl bonds is visible. In the range from 1040

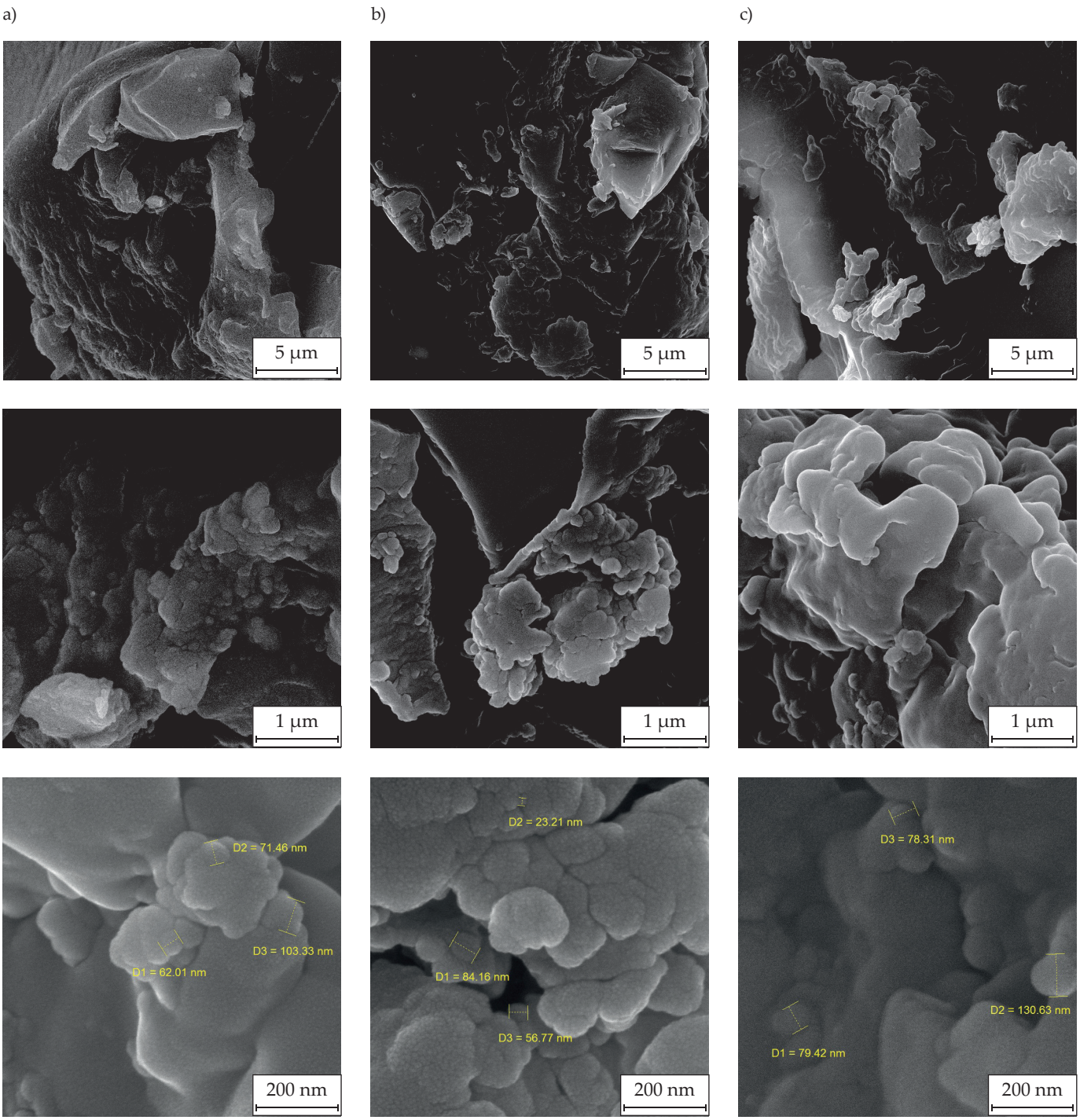

Fig. 9. SEM images of hydrogel containing silver chloride nanoparticles: a) silver nitrate and sodium chloride were added simultaneously, b) silver nitrate was first added, c) sodium chloride was first added

to 1159 cm^{-1}, the observed peaks may be associated with C-OH or C-O-C functional groups.

In the case of hydrogel obtained when silver nintrate was first added, a peak at 481 cm^{-1} is observed, which is not visible in the other hydrogels. In these samples, a peak at 2850 cm^{-1} corresponding to the C-H bonds stretching vibrations is observed that it is not visible in the sample obtained when silver nintrate was first added.

XRD and SEM analysis of hydrogels

To identify and confirm the structure of the obtained products, X-ray diffraction (XRD) and scanning electron microscope (SEM) images were taken with high resolution (Fig. 7).

In the XRD spectrum of a simple hydrogel, the number of peaks and their intensity decreased. In the spectrum of the

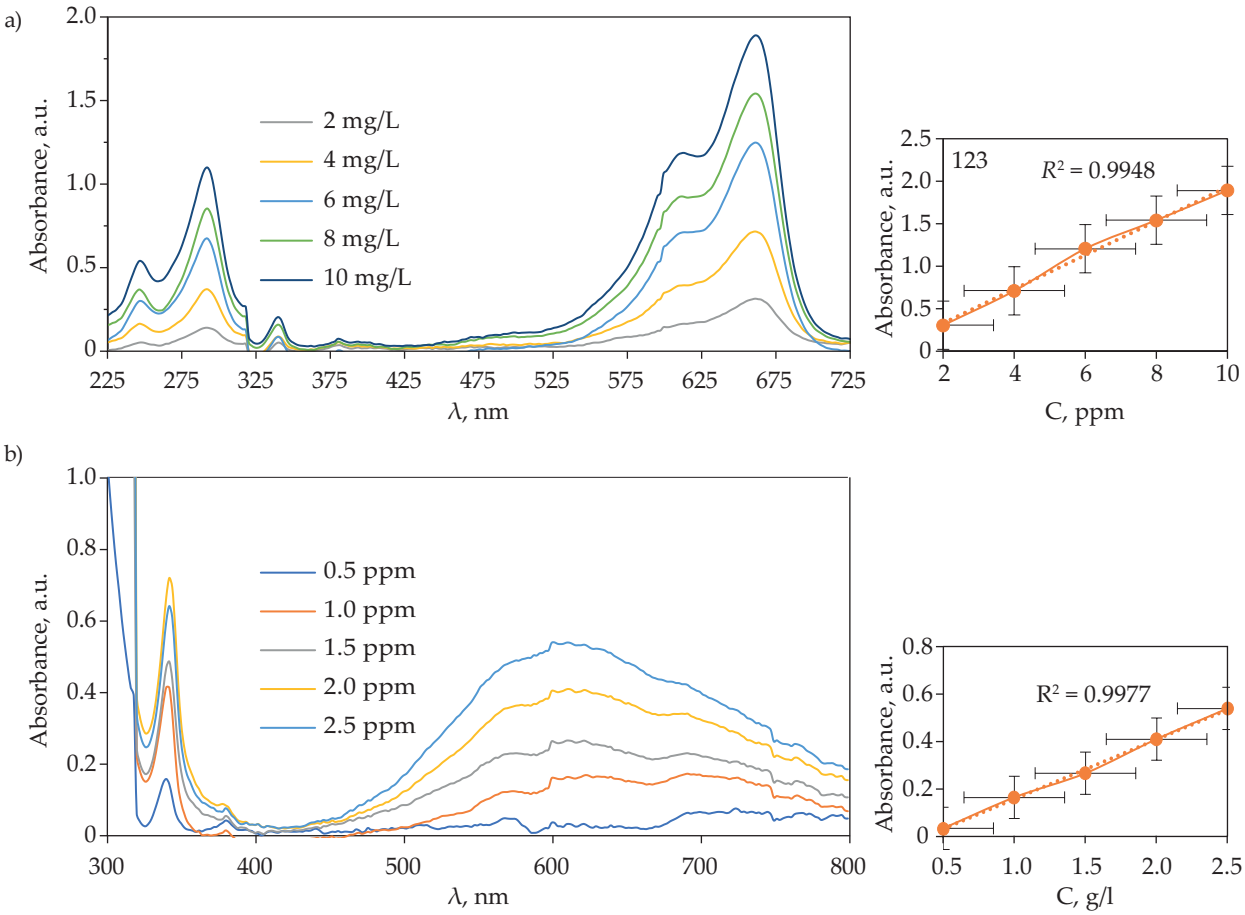

Fig. 10. Absorption spectra of: a) methylene blue and b) copper(II) solutions, and calibration curves

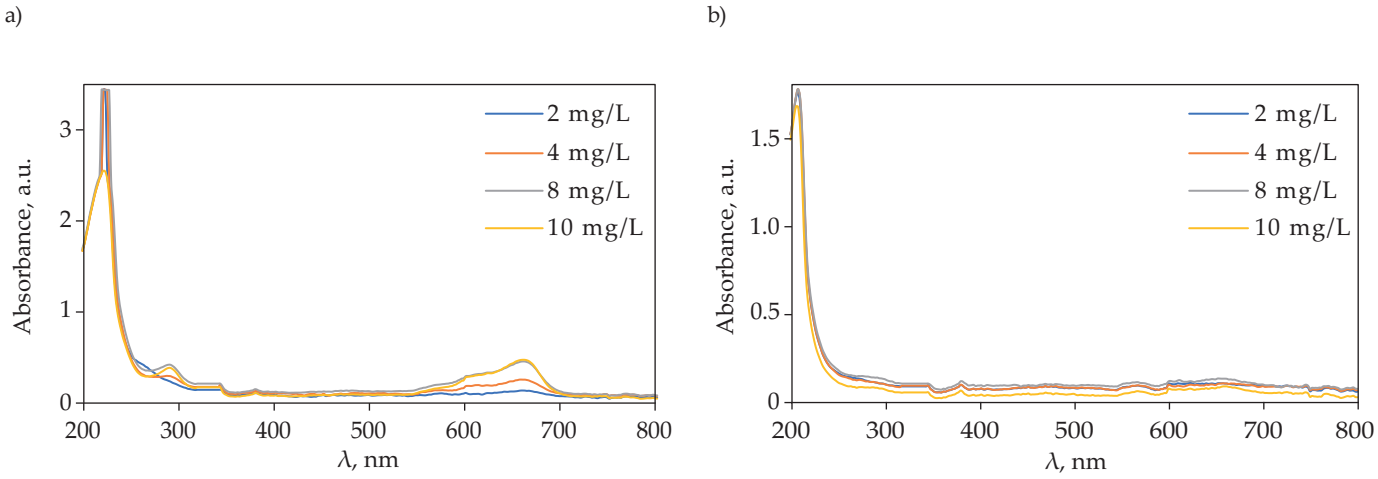

Fig. 11. Reduction of absorption of methylene blue with different initial concentrations after 1h mixing with: a) simple hydrogel and b) Fe_3O_4/gel nanocomposite

hydrogel-containing starch, the peaks are sharp and of high intensity, which indicates its semi-crystalline structure. In the spectrum of hydrogels containing Fe_3O_4 and ZnSe, the number of peaks is smaller and their intensity is the same as in the case of a simple hydrogel, which indicates the interaction of nanoparticles with the polymer matrix.

Figure 8 shows SEM images of a simple hydrogel (Fig. 8a) and hydrogels containing nanoparticles (Fig. 8b-d) differing in size and shape. The images show a uniform distribution of approximately 40 nm nanoparticles that form aggregates of 200 nm.

SEM images of hydrogels containing silver chloride show that higher porosity of the gel is associated with higher absorption of nanoparticles (Fig. 9). When silver nitrate was first added (sample B) significantly more pores are formed, in comparison with the sample when

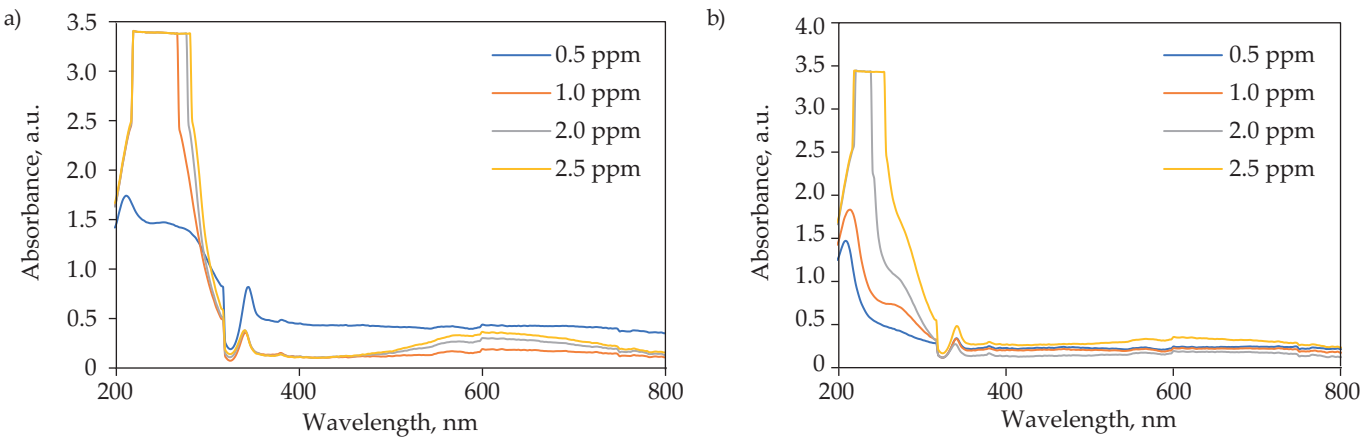

Fig. 12. Reduction of Cu^{2+}absorption after 1h mixing with: a) hydrogel and b) Fe_3O_4/gel nanocomposite

silver nitrate and sodium chloride were added simultaneously (sample A). Sample obtained when sodium chloride was first added (sample C) shows the least number of pores. Depending on the number of pores, the samples are arranged in order B > A > C.

When the silver ions are added first, the only sites that can be coordinated are oxygen groups in the hydrogel. In this slow process, silver ions can penetrate the structure and cavities of the hydrogel. Further, by adding chlorine ions, owing to the small radius and high mobility in comparison to silver ions, quickly penetrate the structure and react with silver ions to produce AgCl. Majority of silver ions loosen their bonds with oxygen groups and participate in the formation of AgCl nanostructures. Due to the availability of oxygen groups (coordinated with silver ions), chlorine atoms create AgCl nanostructures inside hydrogel matrix as a secondary phase. In case of chlorine ions are added before silver ions, or even at a simultaneous time, there would be no opportunity for silver ions to penetrate the hydrogel cavities, and AgCl was quickly precipitated on the surface. The hydrogel nanocomposites were separated from the solution, washed, and dried at 70°C for 12 h.

SEM images also confirmed that, when silver ions are first added, the formation of silver chloride inside the cavities causes the crack formation on the hydrogel surface. In two other samples, the bulk structure of the hydrogel is not changed and AgCl is formed only on the surface (very bright points that turn white).

Pollutant absorption

To study the absorption of organic (methylene blue) and inorganic (Cu^{2+}) pollutants, two hydrogels and two absorbing agents were selected, and their UV-Vis spectra were obtained in the range of 200–800 nm (Fig. 10). The wavelengths of 210 and 260 nm correspond to the n→π* transfer of carbonyl groups -$CONH_2$ and -COOH in the hydrogel structure. No new absorption peaks were observed in the prepared hydrogel compared to the constituent monomers. Therefore, the unsaturated carbonyl system has not changed. The absorbance at 292 and 662 nm is characteristic of methylene blue, and at 342 and 612 nm of copper cations. The concentration of absorbed substances was determined based on calibration curves: for the absorption of methylene blue in the concentration range of 2–10 mg/L (662 nm) and copper cations in the concentration range of 0.5–2.5 ppm (612 nm) (Fig. 10).

During the absorption of methylene blue into the acrylic hydrogel and its nanocomposite, the color of the solution was stable after stirring for 60 min (Fig. 11). This time has been given in the literature as 30 minutes, 200 minutes, and sometimes even up to 400 minutes. A significant change in pH caused by a decrease in H^+ concentration was also observed [21–23]. All copper ions were absorbed into the hydrogel at a concentration of 2 mg/L, while at higher concentrations some of the ions remained in solution. A hydrogel containing magnetic nanoparticles would be more effective in this process and would absorb all copper ions at all selected concentrations.

60 minutes after the time that hydrogel and Fe_3O_4/gel nanocomposite were mixed, the absorption intensity of Cu^{2+} solutions were investigated (Fig. 12). After this time, for all selected concentrations, all copper ions are absorbed into the hydrogel. It is reported that a gel containing magnetic nanoparticles is more effective in this process [24].

CONCLUSIONS

Using ultrasound, polyacrylate hydrogels containing starch, ZnSe, Fe_3O_4 and AgCl nanoparticles were obtained. IR, XRD and SEM studies showed that hydrogels have a uniform porous structure that facilitates the absorption of inorganic and organic pollutants from wastewater. Moreover, silver chloride nanoparticles can form in the cavities of hydrogels. The advantage of the developed hydrogels is their stability and reusability.

REFERENCES

[1] Abdollahi Paynavandi M., Ebrahimi R., Amiri A: *Iranian Journal of Polymer Science and Technology* **2015**, *232*, 28. https://doi.org/10.22063/jipst.2015.1258

[2] Wang L., Zhang J., Wang A.: *Colloids and Surfaces A: Physicochemical and Engineering Aspects* **2008,** *322*, 47. https://doi.org/10.1016/j.colsurfa.2008.02.019

[3] Malatji N., Makhado E., Modibane K.D. *et al.*: *Nanomaterials Nanotechnology* **2021**, *11*, 1. https://doi.org/10.1177/18479804211039425

[4] Ahmed E.M.: *Journal of Advance Research* **2015**, *6*, 105. https://doi.org/10.1016/j.jare.2013.07.006

[5] Darban Z., Shahabuddin S., Gaur R., *et al.*: *Gels* **2022,** *8*, 263. https://doi.org/10.3390/gels8050263

[6] Landers R., Hübner U., Schmelzeisen R. *et al.*: *Biomaterials* **2002**, *23*, 4437. https://doi.org/10.1016/S0142-9612(02)00139-4

[7] Pandey K.K.: *Materials Today: Proceedings* **2021**, *47*, 1520. https://doi.org/10.1016/j.matpr.2021.03.193

[8] Salem W., Leitner D.R., Zingl F.G. *et al.*: *International Journal of Medicine Microbiology* **2015**, *305*, 85. https://doi.org/10.1016/j.ijmm.2014.11.005

[9] Afzal S., Zahid M., Nimra S.S. *et al.*: *Journal of Modeling Polymer Chemistry Materials* **2022,** *1*, 2. https://www.doi.org/10.53964/jmpcm.2022002

[10] Jasim L., Aljeboree A.: *Caspian Journal Environmental Sciences* **2021**, *19*, 789. https://doi.org/10.22124/cjes.2021.5209

[11] Malatji N., Makhado E., Modibane K.D. *et al.*: *Nanomaterials Nanotechnology* **2021**, *11*, 1. https://doi.org/10.1177/18479804211039425

[12] Salama A.: *International Journal of Biology Macromolecules* **2018**, *106*, 940. https://doi.org/10.1016/j.ijbiomac.2017.08.097

[13] Faghani H.A., Heshmati Jannat Magham A.: *Journal of Soil water Conservation* **2019**, *26*, 109. https://doi.org/10.22069/JWSC.2019.15762.3094

[14] Pooresmaeil M., Mansoori Y., Mirzaeinejad M. *et al.*: Adv*ance Polymer Technology* **2018**, *37*, 262. https://doi.org/10.1002/adv.21665

[15] Khan T.A., Nazir M., Ali I. *et al.*: *Arabian Journal of Chemistry* **2017**, *10*, S2388. https://doi.org/10.1016/j.arabjc.2013.08.019

[16] Li J., Fang L., Tait W.R. *et al.*: *RSC Advance* **2017**, *7*, 54823. https://doi.org/10.1039/C7RA10788A

[17] Zhang C., Dai Y., Wu Y. *et al.*: *Carbohydrate Polymer* **2020**, 234, 115882. https://doi.org/10.1016/j.carbpol.2020.115882

[18] Makhado E., Pandey S., Modibane K.D. et al.: *International Journal of Biology Macromolecules* **2020**, *162*, 60. https://doi.org/10.1016/j.ijbiomac.2020.06.143

[19] Hosseini H., Zirakjou A., McClements D.J. *et al.*: *Journal of Hazard Materials* **2022**, *421*, 126752. https://doi.org/10.1016/j.jhazmat.2021.126752

[20] Azzam E.M.S., Elsofany W.I., Alrashdi G.K. *et al.*: *Arabian Journal of Chemistry* **2022**, *15*, 103897. https://doi.org/10.1016/j.arabjc.2022.103897

[21] Salunkhe B., Schuman T.P., *Macromolecules* **2021**, *1*, 256. https://doi.org/10.3390/macromol1040018

[22] Lebkiri I., Abbou B., Kadiri L. *et al.*: *Mediterr Journal of Chemistry* **2019**, *9*, 1. https://doi.org/10.5004/dwt.2021.27530

[23] Ullah A., Zahoor M., Ud Din W. *et al.*: *Adsorption Science Technology* **2022**. https://doi.org/10.1155/2022/5713077

[24] Eldeeb T.M., El-Nemr A., Khedr M.H. *et al.*: *Egyptian Journal of Aquatic Research* **2021**, *47*, 261. https://doi.org/10.1016/j.ejar.2021.07.002

Received 16 IV 2023.